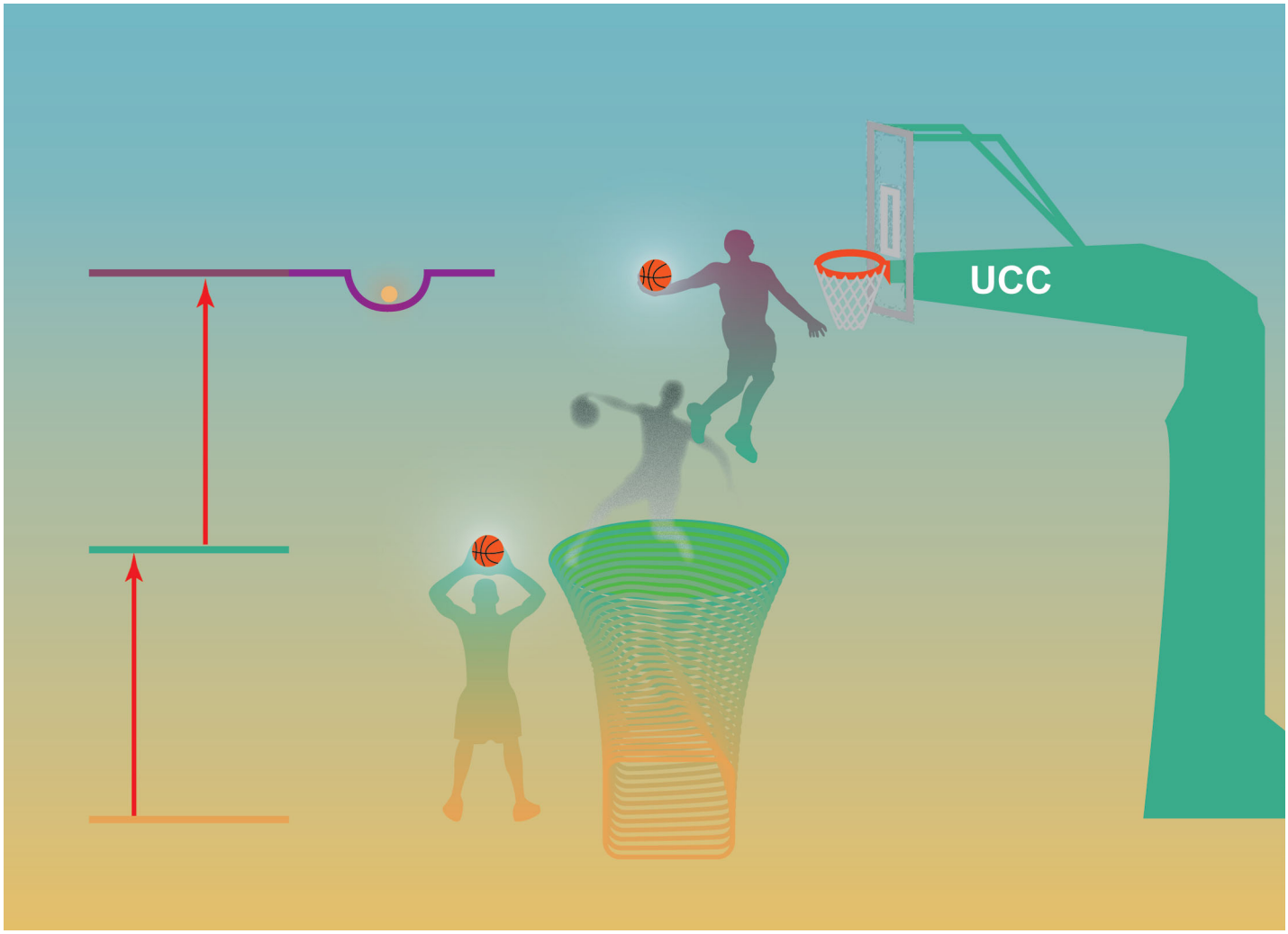

Showcasing research from the University of Georgia (College of Engineering), and Northeast Normal University (Key Laboratory for UV-Emitting Materials and Technology of Ministry of Education).

A new up-conversion charging concept for effectively charging persistent phosphors using low-energy visible-light laser diodes

We report an up-conversion charging (UCC) technique, which offers a new way to study persistent luminescence and utilize persistent phosphors.

As featured in:

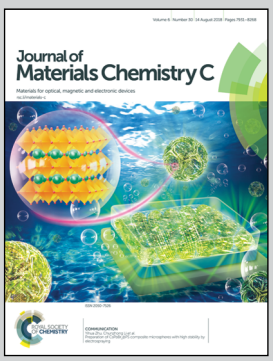

See Feng Liu, Zhengwei Pan *et al.*, *J. Mater. Chem. C*, 2018, **6**, 8003.

ROYAL SOCIETY OF CHEMISTRY

rsc.li/materials-c

Registered charity number: 207890

Journal of Materials Chemistry C

PAPER

View Article Online
View Journal | View Issue

Cite this: J. Mater. Chem. C, 2018, 6, 8003

A new up-conversion charging concept for effectively charging persistent phosphors using low-energy visible-light laser diodes†

Yafei Chen,[ab] Feng Liu, *[acd] Yanjie Liang,[ab] Xianli Wang,[a] Jianqiang Bi,[b] Xiao-jun Wang[e] and Zhengwei Pan *[ac]

Received 18th May 2018,
Accepted 16th June 2018

DOI: 10.1039/c8tc02419g

rsc.li/materials-c

It is general knowledge in persistent luminescence that high-energy illumination, mostly ultraviolet light, is usually necessary in order to effectively charge persistent phosphors. However, the need for high-energy ultraviolet light excitation compromises some applications. In his pioneering work on ruby (Al_2O_3:Cr^{3+}) laser materials in 1960, Theodore Maiman observed an excited-state absorption phenomenon under the excitation of a high-intensity green-light flash tube. Inspired by Maiman's observation, here we propose a new two-photon up-conversion charging (UCC) concept to effectively charge Cr^{3+}-activated near-infrared persistent phosphors using low-energy, high-intensity visible-light laser diodes. As an example, we demonstrate that a low-energy 635 nm laser diode can produce persistent luminescence in the $LiGa_5O_8$:Cr^{3+} persistent phosphor at the same magnitude as that produced by high-energy 335 nm ultraviolet light from a xenon arc lamp. Moreover, the UCC appears to be a common phenomenon in persistent phosphors containing other UCC-enabling activators such as rare-earth Pr^{3+} ions and transition metal Mn^{2+} ions. The UCC technique offers a new way to study persistent luminescence and utilize persistent phosphors; for instance, in bioimaging it makes effective *in vivo* charging persistent optical probes using tissue-friendly visible light possible.

Introduction

Persistent luminescence, also called afterglow, is a special optical phenomenon in which the emission in a persistent phosphor can last for hours after ceasing the excitation.[1,2] Based on an electron transfer assumption, for a persistent phosphor to maximally exhibit its persistent luminescence potential, the electron traps in the material, which usually locate close to the bottom of the conduction band, need to be fully filled upon an ionizing excitation *via* the conduction band state.[3–9] Accordingly, in research and practical applications, high-energy ultraviolet (UV) light (mostly 250–400 nm), including the UV light from mercury UV lamps, xenon arc lamps and the Sun, is consistently used to charge persistent phosphors. However, the need for high-energy UV light excitation compromises some applications, such as bioimaging,[10,11] where the UV light is unsuitable or harmful. Therefore, the ability to achieve effective charging using low-energy light, such as visible light or near-infrared (NIR) light, is highly desirable and was identified as a grand challenge in the field.[12] Recently, a few charging techniques using low-energy NIR laser diodes (*e.g.*, 808 nm and 980 nm laser diodes) were developed to charge Cr^{3+}-activated persistent phosphors.[13,14] Despite the progress, the persistent luminescence produced by these charging techniques is relatively weak for practical applications. To make low-energy light charging meaningful, the persistent luminescence performance (*i.e.*, persistent luminescence intensity and duration) of a persistent phosphor charged by a low-energy light source needs to reach the magnitude produced by the common high-energy UV light sources (*e.g.*, xenon lamps or mercury UV lamps).

A trivalent chromium (Cr^{3+}) ion with d^3 electron configuration is well known for its broadband absorption in the UV-to-visible spectral region in phosphors. Crystals doped with Cr^{3+} ions have numerous optical and spectral applications, with the most famous one being the ruby crystal (Al_2O_3:Cr^{3+}) – on which Maiman realized

[a] College of Engineering, University of Georgia, Athens, GA 30602, USA. E-mail: panz@uga.edu, fengliu@nenu.edu.cn
[b] Key Laboratory for Liquid–Solid Structure Evolution and Processing of Materials, Shandong University, Jinan 250061, China
[c] Department of Physics and Astronomy, University of Georgia, Athens, GA 30602, USA
[d] Key Laboratory for UV-Emitting Materials and Technology of Ministry of Education, Northeast Normal University, Changchun 130024, China
[e] Department of Physics, Georgia Southern University, Statesboro, GA 30460, USA

† Electronic supplementary information (ESI) available: NIR imaging, calculation of safe exposure limits, table of safe exposure limits, UCC decay, UCC decay curves charged by a 635 nm laser diode, excitation power dependence, excitation duration dependence, UCC imaging, persistent luminescence excitation spectra, and laser power of the laser diode. See DOI: 10.1039/c8tc02419g

the first working laser in 1960 through exciting the crystal using a high-intensity green-light (~560 nm) flash tube.[15] In recent years, Cr^{3+}-activated, gallate-based NIR persistent phosphors (*e.g.*, $LiGa_5O_8:Cr^{3+}$, $Zn_3Ga_2Ge_2O_{10}:Cr^{3+}$, and $ZnGa_2O_4:Cr^{3+}$)[16–18] have attracted considerable attention because of their promising applications in bioimaging and night-vision applications. While the photoluminescence of these Cr^{3+}-activated phosphors can be effectively excited by both the UV and visible light (~250–680 nm) of a xenon lamp, their persistent luminescence can only be effectively produced by the high-energy UV light.[16,17] This phenomenon is understandable because individual visible-light photons from the low-intensity xenon lamp cannot reach the high-energy delocalization state (*i.e.*, an excited state associated with delocalization properties) of $Cr^{3+}$to fill the electron traps.

However, the knowledge obtained from the low-intensity xenon lamp excitation is one-sided. In Maiman's pioneering work, he also observed an excited-state absorption phenomenon in ruby.[19] That is, the green flash light excitation firstly populated the ^2E level of Cr^{3+} ions, and during the long lifetime (~5 ms) of the ^2E metastable state a second green excitation photon further raised the Cr^{3+} ion to a higher-lying charge transfer state. This observation clearly indicated the occurrence of transitions between two excited optical states of Cr^{3+} under intense green light excitation. However, this excited-state absorption in ruby did not receive much attention and further study, because often this type of excited-state absorption prevents a material from becoming a good laser material; that is, the second excitation step decreases the population inversion that is essential for achieving laser radiation.

Although the excited-state absorption phenomenon in ruby is undesirable for laser applications, it inspires us to speculate that it may provide a promising solution to effectively charge the Cr^{3+}-activated persistent phosphors using low-energy, high-intensity visible light sources, such as visible-light laser diodes. We therefore propose a new, two-photon up-conversion charging (UCC) concept to effectively charge Cr^{3+}-activated persistent phosphors using a visible-light laser diode, as schematically depicted in Fig. 1a. In the UCC concept, the first absorption of a visible-light photon excites the system to the $^4T_2$ state (*i.e.*, the intermediate state) of Cr^{3+} ions, followed by a fast non-radiative relaxation to the ^2E emitting state. The ^2E level can be regarded as a metastable state because of its long stable-state luminescence lifetime (usually >1 ms).[19,20] The high pumping intensity of the laser diode enables the population of the metastable state to be high enough to produce substantial excited state absorption. Such an excited metastable state can successively absorb another visible-light photon to further pump the system to the high-energy $^4T_1(^4P)$ state. Subsequently, the electrons will delocalize with a significant probability from the $^4T_1(^4P)$ state (*via* an autoionization process) and then fill the electron traps. In this article, we use a $LiGa_5O_8:Cr^{3+}$ NIR persistent phosphor[16] as a representative material to demonstrate the UCC process as well as the related UCC properties.

Experimental

Materials synthesis

The $LiGa_5O_8:Cr^{3+}$ phosphor discs (15 mm in diameter and 1 mm in thickness) were fabricated using a solid-state reaction method as described in ref. 16.

The $LiGa_5O_8:Cr^{3+}$ nanoparticles were synthesized using a combustion method *via* a highly exothermic redox reaction between metal nitrates and organic fuels. The synthesis procedure is briefly described as follows. A solution was prepared by dissolving a stoichiometric amount of lithium nitrate ($LiNO_3$, 99%), gallium nitrate [$Ga(NO_3)_3$, 99.999%] and chromium nitrate [$Cr(NO_3)_3$, 98.5%] in a minimum amount of deionized

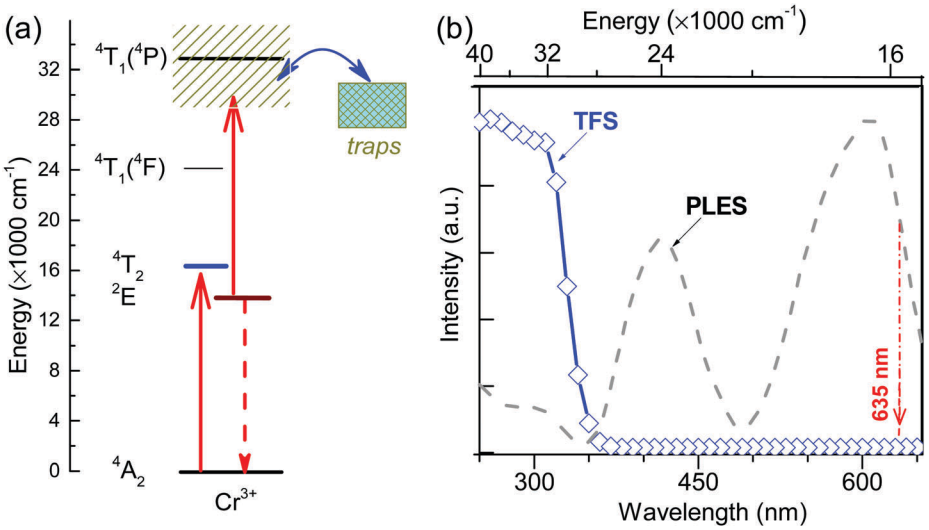

Fig. 1 UCC concept in a Cr^{3+}-activated persistent luminescence system. (a) Schematic diagram of the two-photon UCC process in a Cr^{3+}-activated persistent luminescence system under the excitation of a visible-light laser diode. The diagonal region represents the delocalization state. Straight-line arrows and curved-line arrows represent optical transitions and electron transfer processes, respectively. (b) Photoluminescence excitation spectrum (PLES) and persistent luminescence excitation spectrum (*i.e.*, trap filling spectrum, TFS) of the $LiGa_5O_8:Cr^{3+}$ persistent phosphor.

water in a crystallizing dish. Certain amounts of organic fuels glycine and carbonhydrazide (molar ratio 5 : 2) were then added to the solution. The solution was heated at 60 °C with continuous and mild stirring on a stirring hotplate to slowly evaporate the water. Once the water was evaporated, a transparent gel was formed. The gel was then transferred to a 600 °C muffle oven, where the organic fuels and metal nitrides were ignited and reacted to burn to yield white, voluminous and foamy $LiGa_5O_8:Cr^{3+}$ phosphor. The foamy $LiGa_5O_8:Cr^{3+}$ product was then crashed and ultrasonically dispersed in deionized water. After centrifugation and filtration, $LiGa_5O_8:Cr^{3+}$ nanoparticles with diameters in the range of 50–150 nm were obtained.

The $MgGeO_3:Pr^{3+}$ and $MgGeO_3:Mn^{2+}$ persistent phosphors were fabricated using a solid-state reaction method. The source materials for the $MgGeO_3:Pr^{3+}$ phosphor are MgO, GeO_2 and $PrCl_3$ powders (the Pr^{3+} concentration is 0.1 mole%). The source materials for the $MgGeO_3:Mn^{2+}$ phosphor are MgO, GeO_2 and MnO powders (the Mn^{2+} concentration is 1 mole%). For each phosphor, stoichiometric amounts of source powders were thoroughly mixed and ground into a homogenous fine powder in an agate mortar. The mixed powder was pressed into discs (~15 mm in diameter and ~1 mm in thickness) using a 16 T dry pressing machine. The discs were then sintered at 1250 °C for $MgGeO_3:Pr^{3+}$ and $MgGeO_3:Mn^{2+}$ in air for 2 h to form the final ceramic products.

Spectroscopic measurements

The spectral properties (decay curves and persistent luminescence emission spectra) of $LiGa_5O_8:Cr^{3+}$, $MgGeO_3:Pr^{3+}$ and $MgGeO_3:Mn^{2+}$ persistent phosphors were measured using a Horiba FluoroLog-3 spectrofluorometer equipped with a 450 W xenon arc lamp and a R928P photomultiplier tube (240–850 nm). Three visible-light laser diodes were used in the UCC experiments: a power-tunable (0–1000 mW) 635 nm laser diode, a 1000 mW 450 nm laser diode, and a 200 mW 532 nm laser diode. A Thorlabs PM100D power energy meter (200–1100 nm) was used to measure the power density of the xenon lamp and laser diodes. All spectra were corrected for the optical system responses. Appropriate optical filters were used to avoid stray light in spectral measurements. Before all the spectral measurements, the samples were heat-treated in a muffle oven at 400 °C for 15 min to completely empty the traps. For Fig. 3 and 5a, the persistent luminescence intensity (*i.e.*, I_{30s}) was recorded at 30 s after ceasing each excitation.

Results and discussion

The measurements were carried out on $LiGa_5O_8:Cr^{3+}$ phosphor discs (15 mm in diameter and 1 mm in thickness) with Cr^{3+} concentration at 1 atom%. Under the excitation of a filtered 450 W xenon lamp, the NIR photoluminescence (peaking at 716 nm) of the $LiGa_5O_8:Cr^{3+}$ phosphor can be produced by both UV light and visible light excitations; however, its NIR persistent luminescence can only be achieved by high-energy UV light (<360 nm) excitation,[16] as the photoluminescence excitation spectrum (PLES) and the persistent luminescence excitation spectrum (*i.e.*, the trap filling spectrum, TFS) show in Fig. 1b. When a high-intensity visible-light laser diode is used as the excitation source, according to the UCC concept in Fig. 1a, the occurrence of the UCC process of Cr^{3+} ions should consist of two excitation steps. The first excitation step is from the ground state $^4A_2$ to the metastable excited state ^2E and the second excitation step is from the ^2E state to the high-energy delocalized state $^4T_1(^4P)$. It is expected that the excitability of the first excitation step is related to the photoluminescence excitation behavior (*i.e.*, the PLES in Fig. 1b) of the phosphor, which suggests that high-intensity visible light in the ranges of ~400–480 nm and of ~510–650 nm can generate substantial population in the ^2E state. Since the ^2E state is the starting state for the second excitation step, it is expected that high-intensity visible light with energy higher than the energy difference between the ^2E state (14 100 cm^{-1}) and the $^4T_1$ state (~28 000 cm^{-1}), which is ~13 900 cm^{-1} or ~719 nm, can pump the system from the metastable ^2E state to the high-energy $^4T_1(^4P)$ state. Based on the excitability of the two excitation steps, we speculate that high-intensity visible light with wavelengths of ~400–480 nm and ~510–650 nm is capable of effectively charging the $LiGa_5O_8:Cr^{3+}$ phosphor *via* the UCC process and therefore producing strong persistent luminescence.

To test our speculation and the UCC concept, we excited the $LiGa_5O_8:Cr^{3+}$ phosphor using three widely used visible-light laser diodes with emission wavelengths of 450 nm, 532 nm and 635 nm. As expected, all these three visible-light laser diodes can effectively charge the $LiGa_5O_8:Cr^{3+}$ phosphor and produce intense, long-lasting (>50 h) Cr^{3+} persistent luminescence after a short duration (*e.g.*, 10 s) excitation, as the persistent luminescence decay curves show in Fig. 2a for 635 nm laser diode excitation and Fig. S1 (ESI†) for 450 nm and 532 nm laser diode excitations. The persistent luminescence intensities and durations produced by these visible-light laser diodes are at the same magnitude as that produced by the UV light from a xenon lamp or a mercury UV lamp.[16] Fig. 2b shows the persistent luminescence emission spectrum recorded at 1 h after ceasing the 635 nm laser diode excitation, showing characteristic Cr^{3+} emission. Below, we focus on the results obtained by using a power-tunable (0–1000 mW) 635 nm laser diode excitation.

To understand the UCC process in the $LiGa_5O_8:Cr^{3+}$ phosphor under 635 nm laser diode excitation, we studied the relationship between the laser output power and the persistent luminescence performance. The phosphor was irradiated using the laser diode with the output powers tuning from 0.2 mW to 800 mW for a fixed excitation duration (*e.g.*, 10 s, 30 s, 60 s or 300 s), and persistent luminescence decay curves monitoring at 716 nm were recorded after each excitation. Fig. S2 (ESI†) shows the persistent luminescence decay curves acquired for excitations with a excitation duration of 10 s. Using the persistent luminescence intensity at 30 s after ceasing each excitation as the reference point, a plot of persistent luminescence intensity (I_{30s}) *versus* the laser output power (P) is obtained, as shown by the I–P plot in Fig. 3a. Fig. 3a and Fig. S2 (ESI†) show that in order to generate detectable (by the FluoroLog-3 spectrofluorometer) persistent luminescence in the $LiGa_5O_8:Cr^{3+}$ phosphor, the output power

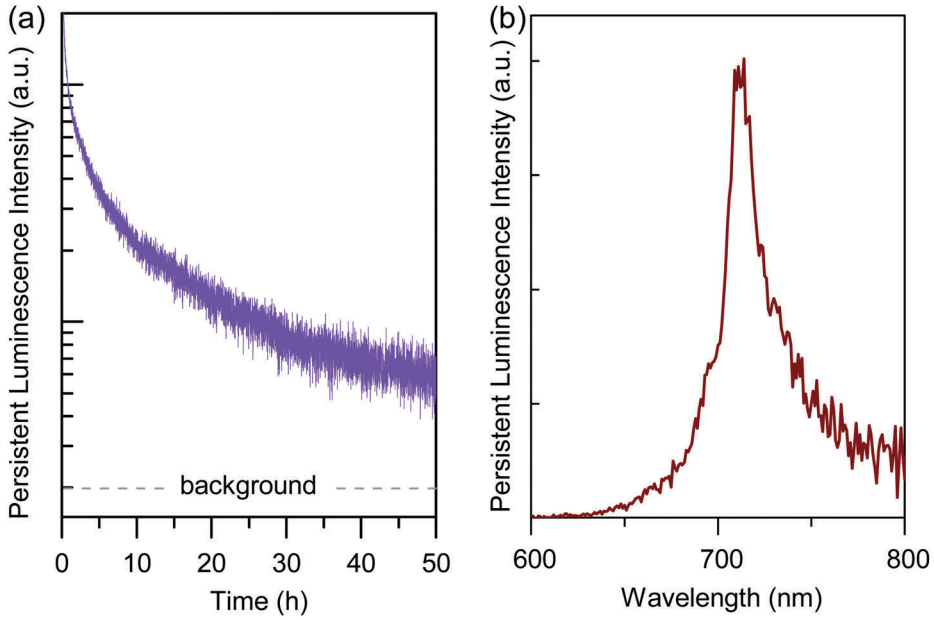

Fig. 2 UCC induced persistent luminescence in the $LiGa_5O_8:Cr^{3+}$ persistent phosphor. (a) UCC induced persistent luminescence decay curve after excitation by a 635 nm laser diode at 600 mW for 10 s. The decay is monitored at Cr^{3+} 716 nm emission. (b) UCC persistent luminescence emission spectrum recorded at 1 h after ceasing the excitation.

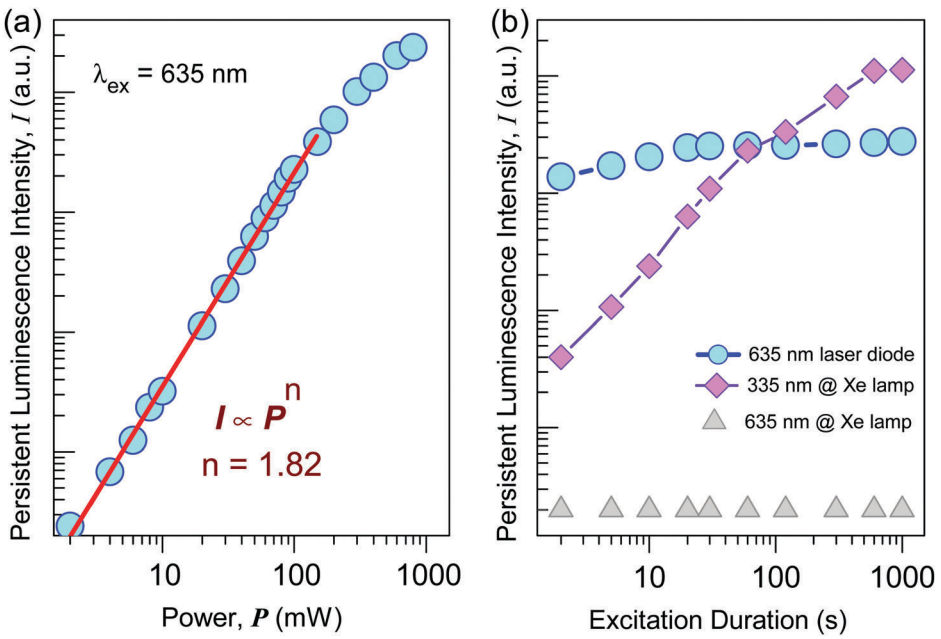

Fig. 3 Excitation power and excitation duration dependent UCC persistent luminescence intensity in the $LiGa_5O_8:Cr^{3+}$ persistent phosphor. (a) Double-logarithmic plot of UCC persistent luminescence intensity *versus* excitation power of a 635 nm laser diode. The excitation duration is 10 s for each excitation. The red line is the quadratic fit of the plot. (b) Excitation duration dependent UCC persistent luminescence intensity excited by a 635 nm laser diode at 600 mW and by a filtered 450 W xenon lamp at 635 nm and 335 nm. In both cases, the persistent luminescence was monitored at Cr^{3+} 716 nm emission.

of the 635 nm laser diode should be higher than ~2 mW (corresponding to a power intensity of ~20 mW cm^{-2} incident on the sample), and the persistent luminescence intensity increases as the power increases. By fitting the *I–P* plot in Fig. 3a, a quadratic relationship, *i.e.*, $I–P^{1.82}$, is obtained for the excitation power in the range of 2–100 mW. A similar *I–P* relationship was also obtained when the excitation duration was 30 s, 60 s or 300 s (Fig. S3, ESI†). Such a quadratic *I–P* relationship clearly reveals that two 635 nm photons are absorbed in order to pump the Cr^{3+} system to the high-energy delocalization state, which perfectly verifies the two-photon UCC concept in Fig. 1a.

The *I–P* plot in Fig. 3a also shows that when the output power is higher than ~100 mW, the slope of the *I–P* plot decreases as the power increases (a similar relationship also occurs for longer excitation durations; see Fig. S3, ESI†). Besides the well-known saturation effect[21] during the up-conversion excitation, a photostimulation effect, *i.e.*, while filling the electron traps, the excitation light can also simultaneously pump-out some captured electrons from the traps,[13] is believed to also significantly contribute to the decrease of the slope.

To evaluate the effectiveness of the UCC process, we compared the persistent luminescence generated by the 635 nm laser diode with that produced by an equivalent high-energy UV light from the filtered 450 W xenon lamp. The equivalent UV light is the one that can linearly excite the system to the same high-energy delocalization state as the two up-converting 635 nm photons do. According to Fig. 1a, the equivalent excitation energy equals to the sum of the energy of the metastable level of Cr^{3+} (14 100 cm^{-1}) and the energy of the second 635 nm photon (15 750 cm^{-1}), which is 29 850 cm^{-1} or 335 nm. Fig. 3b shows the persistent luminescence intensity as a function of the excitation duration (2 s to 1000 s) in the $LiGa_5O_8:Cr^{3+}$ phosphor using two excitation sources: a 635 nm laser diode with 600 mW output power (lower output powers in the range of 10–150 mW were also used; see Fig. S4, ESI†) and a 450 W xenon lamp with wavelengths of 335 nm and 635 nm. The excitation intensities of the 335 nm and 635 nm xenon light incident on the sample are ~1 mW cm^{-2} and ~0.18 mW cm^{-2}, respectively. Although the low-intensity 635 nm light from the xenon lamp cannot fill the electron traps to produce persistent luminescence in $LiGa_5O_8:Cr^{3+}$ at all, the high-intensity 635 nm light from the laser diode can, and the trap filling process proceeds surprisingly fast. With about 20 s irradiation the charging appears to become saturated for the 600 mW output power (it takes longer time to saturate for lower output powers; see Fig. S4, ESI†). The intensity of the persistent luminescence produced by the 600 mW 635 nm laser diode excitation is comparable to that produced by the 335 nm xenon light excitation, indicating that the low-energy, high-intensity red laser diode excitation can effectively fill the electron traps and thus produce intense persistent luminescence in the $LiGa_5O_8:Cr^{3+}$ phosphor.

It is worth mentioning that besides in the $LiGa_5O_8:Cr^{3+}$ ceramic discs discussed above, UCC-induced persistent luminescence also occurs in $LiGa_5O_8:Cr^{3+}$ nanoparticles, as revealed by the NIR persistent luminescence image of $LiGa_5O_8:Cr^{3+}$ nanoparticle colloidal solution in Fig. S5 (ESI†). Moreover, the UCC process can also occur in other Cr^{3+}-activated, gallate-based NIR persistent phosphors such as $Zn_3Ga_2Ge_2O_{10}:Cr^{3+}$.[17]

From the UCC concept and the UCC properties in the $LiGa_5O_8:Cr^{3+}$ persistent phosphor, we found that in order to achieve UCC in a persistent phosphor there are requirements on both the excitation source and the activator ion. For the excitation source, its output power intensity needs to be relatively high (*e.g.*, >20 mW cm^{-2} for the $LiGa_5O_8:Cr^{3+}$ phosphor using a 635 nm laser diode), and its photon energy should be higher than the metastable state energy of the activator ion (*e.g.*, the ^2E level in Cr^{3+}). For the activator ion, two prerequisites are simultaneously required: a long-lifetime metastable state and a high-energy delocalization state. The lifetime of the metastable state should be sufficiently long (*e.g.*, >1 ms), so that a second excitation photon can be promoted from the state during its lifetime. With regard to the delocalization state, the activator ion should have a tendency to be oxidized in solid (*e.g.*, $Cr^{3+} \rightarrow Cr^{4+}$), so that the electron transfer process can take place between the activator ion and the electron traps. According to these two prerequisites, we expected that some other activator ions, such as rare-earth Pr^{3+} ions and transition metal Mn^{2+} ions (Fig. 4a), should also exhibit the UCC phenomenon when doped in appropriate hosts. We then fabricated a series of persistent phosphors containing Pr^{3+} and Mn^{2+} ions, such as $MgGeO_3:Pr^{3+}$ and $MgGeO_3:Mn^{2+}$, and indeed observed strong UCC persistent luminescence in these phosphors with the excitation of visible-light laser diodes (Fig. 4b and c). (Note: the persistent luminescence of $MgGeO_3:Pr^{3+}$ and $MgGeO_3:Mn^{2+}$ persistent phosphors can only be produced by the UV light of a xenon lamp; see Fig. S6, ESI†). These results indicate that the UCC is a common phenomenon in persistent phosphors containing UCC-enabling activator ions.

The effective, low-energy visible-light laser diode excitability offered by the UCC is expected to have significant impacts on some applications. For instance, the UCC capability of the NIR-emitting $LiGa_5O_8:Cr^{3+}$ phosphor makes *in vivo* charging the material using tissue-friendly visible light sources possible in medical applications. For using laser diodes in medical applications, limits of exposure to laser radiation were established by the International Commission on Non-Ionizing Radiation Protection (ICNIRP) to avoid causing adverse biological effects to the eye and the skin.[22] The safe exposure limits of a 635 nm laser diode to the skin, which depend on the laser output power and the exposure duration, were calculated using the method provided in the ICNIRP guidelines (see Table S1, ESI†). The calculation shows that for a 635 nm laser diode the safe laser output power to the skin is ≤100 mW (corresponding to ≤1000 mW cm^{-2} in power intensity). When the output power is ≤20 mW, the irradiation is safe for any long exposure duration, while in the range of 20–100 mW, the irradiation is safe only for limited exposure duration (~1–10 s), as shown by the red open circle curve on the base plane in Fig. 5a. We then used the exposure limits to excite the $LiGa_5O_8:Cr^{3+}$ phosphor and recorded persistent luminescence decay curves (monitored at Cr^{3+} 716 nm emission). The persistent luminescence intensity, *i.e.*, I_{30s}, which was determined using the same method as that used for Fig. 3a, was plotted as a function of the laser output power (20–100 mW) and the excitation duration (1–1800 s; 1800 s is the longest duration used in our experiment), as shown by the pink ball curve in Fig. 5a. Fig. 5a shows that within the 20–100 mW power range of a 635 nm laser diode, exciting the $LiGa_5O_8:Cr^{3+}$ phosphor by a large power for a short duration (*e.g.*, 80–100 mW for 1–2 s) and by a small power for a long duration (*e.g.*, 20 mW for >100 s) can both produce considerably high persistent luminescence intensity. Any exposure conditions lower than the exposure limits, as represented by the grid area on the base plane in Fig. 5a, are safe to the skin.

In using the UCC technique to excite the $LiGa_5O_8:Cr^{3+}$ phosphor *in vivo*, while the exposure limits need to be considered, the attenuation of tissues to the laser beam should also be

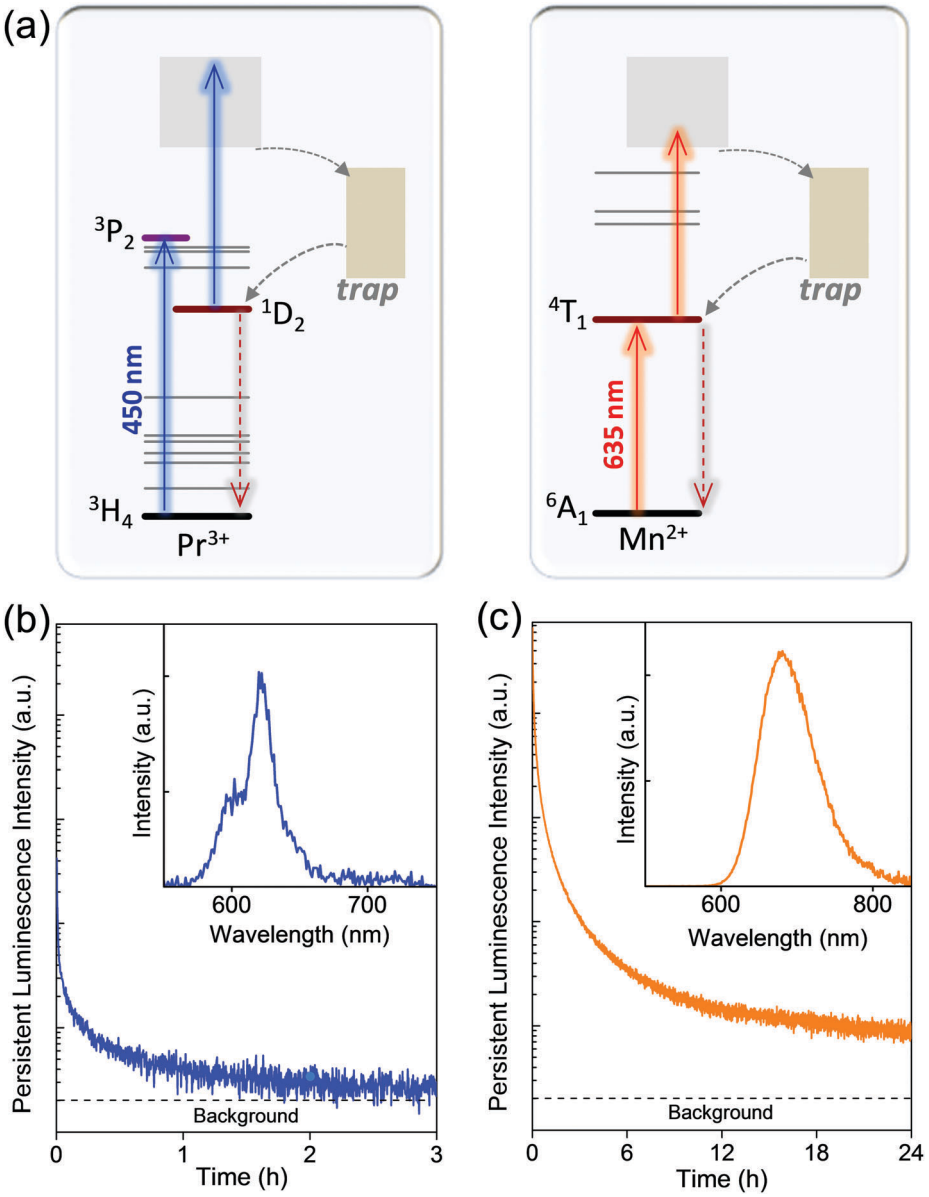

Fig. 4 UCC in Pr^{3+}- and Mn^{2+}-activated persistent luminescence systems. (a) Schematic diagrams of UCC processes in Pr^{3+}- and Mn^{2+}-activated persistent luminescence systems under the excitation of visible-light laser diodes. Diagonal regions represent the delocalization states. Straight-line arrows and curved-line arrows represent optical transitions and electron transfer processes, respectively. (b) UCC induced persistent luminescence decay curve of the $MgGeO_3$:Pr^{3+} phosphor after excitation by a 450 nm laser diode at 1000 mW for 10 s. The decay is monitored at Pr^{3+} 624 nm emission. The inset shows the UCC persistent luminescence emission spectrum recorded at 10 min after ceasing the excitation. (c) UCC induced persistent luminescence decay curve of the $MgGeO_3$:Mn^{2+} phosphor after excitation by a 635 nm laser diode at 600 mW for 10 s. The decay is monitored at Mn^{2+} 678 nm emission. The inset shows the UCC persistent luminescence emission spectrum recorded at 1 h after ceasing the excitation.

considered because, as shown in Fig. 3a, a minimum power of 2 mW is needed in order to produce detectable persistent luminescence (by the FluoroLog-3 spectrofluorometer) in the $LiGa_5O_8$:Cr^{3+} phosphor. Using pork tenderloin as a model tissue, we measured the remaining power of a 635 nm laser diode after the laser beam (1–1000 mW) penetrated 1 to 10 mm thick pork, as shown in Fig. S7 (ESI†). At output powers of 20 mW and 100 mW, the remaining powers of the 635 nm laser diode were expected to be high enough (*i.e.*, >2 mW) to charge the $LiGa_5O_8$:Cr^{3+} phosphor located up to 3 mm and 6 mm, respectively, deep within pork. Indeed, by charging the $LiGa_5O_8$:Cr^{3+} phosphor disc located at 1 mm and 3 mm deep within pork using a 635 nm laser diode at 20 mW for 5 min and at 100 mW for 1 s, respectively, considerably high persistent luminescence was detected in both cases (Fig. 5b). The remaining powers of the 20 mW laser beam passing through 1 mm pork and 100 mW laser beam passing through 3 mm pork are ~6.5 mW and ~8.5 mW, respectively. As expected, the persistent luminescence intensity produced by the remaining laser power is at the same magnitude as that produced by the same power but

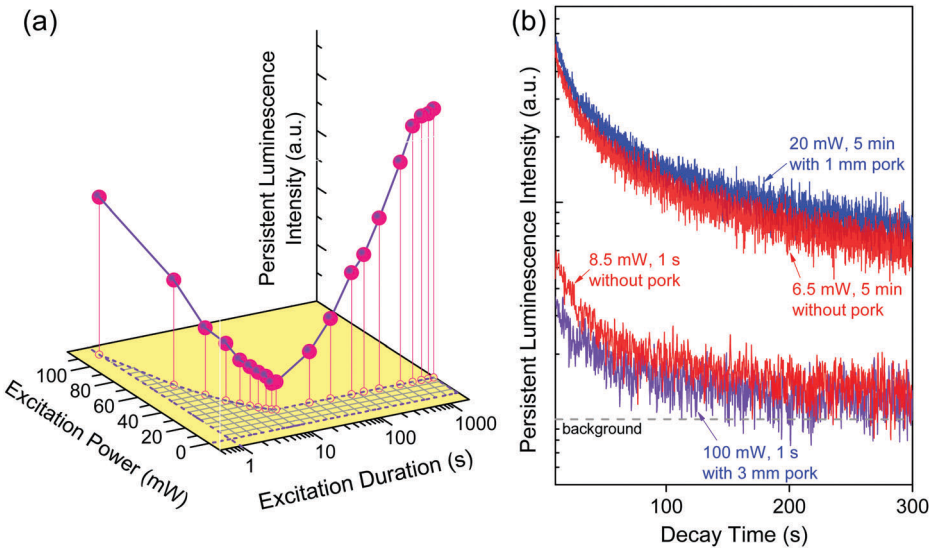

Fig. 5 UCC-induced persistent luminescence in the $LiGa_5O_8:Cr^{3+}$ persistent phosphor after being charged by a 635 nm laser diode within safe exposure power limits. (a) A 3-D graph showing the relationship between the persistent luminescence intensity and the safe exposure limits. The red open circle curve on the base plane represents the safe exposure limits, which depend on the laser output power and the exposure duration. The pink ball curve shows the persistent luminescence intensities (monitored at 716 nm) after the excitation along the exposure limits. The grid area on the base plane represents the safe irradiation conditions for a 635 nm laser diode to the skin. (b) UCC induced persistent luminescence decay curves of the $LiGa_5O_8:Cr^{3+}$ phosphor disc embedded in pork tenderloin after being charged by a 635 nm laser diode at 20 mW for 5 min and at 100 mW for 1 s. Decay curves obtained after excitations by 6.5 mW for 5 min and 8.5 mW for 1 s without pork are also shown. The decay was monitored at Cr^{3+} 716 nm emission.

without the pork. Fig. 5b also shows that the persistent luminescence intensity obtained after irradiation at 6.5 mW for 5 min is significantly higher than that obtained after irradiation at 8.5 mW for 1 s, showing that at similar laser output power, the extent of charging is more effective for longer irradiation duration. Overall, the above studies provide the foundation for medical research and applications that involve charging of the $LiGa_5O_8:Cr^{3+}$ phosphor *in vivo* using a 635 nm laser diode.

Conclusions

We have proposed and investigated a new, two-photon UCC concept to effectively charge persistent phosphors containing UCC-enabling activator ions (including Cr^{3+}, Pr^{3+} and Mn^{2+}) using low-energy, high-intensity visible-light laser diode excitation. The low-energy visible-light excitability offered by the UCC represents a breakthrough in the field of persistent luminescence, which is expected to have significant impacts on both fundamental luminescence research and practical applications of persistent phosphors. For instance, in biomedical research the UCC makes effective *in vivo* charging persistent optical probes using tissue-friendly visible light sources possible. Moreover, since the UCC appears to be a common phenomenon in persistent phosphors containing UCC-enabling activator ions, many existing persistent phosphors that were previously well-studied using UV excitation can now be revisited using visible-light laser diode excitation, enabling new luminescence properties to be discovered and new applications to be developed. Considering the wide use of visible-light laser diodes nowadays and the increasing applications of persistent phosphors in many important fields, the UCC technique offers a new way to study persistent luminescence and utilize persistent phosphors.

Conflicts of interest

There are no conflicts to declare.

Acknowledgements

Z. W. P. acknowledges financial support from the National Science Foundation (DMR-1403929 and DMR-1705707). J. Q. B. thanks the financial support from the National Natural Science Foundation of China (No. 51272132). F. L. thanks the financial support from the National Natural Science Foundation of China (No. 11774046). Y. F. C. and Y. J. L. acknowledge support from the China Scholarship Council.

Notes and references

1 J. Hölsä, *Electrochem. Soc. Interface*, 2009, **18**, 42.
2 W. M. Yen, S. Shionoya and H. Yamamoto, *Phosphor Handbook*, CRC Press/Taylor and Francis, Boca Raton, FL, USA, 2nd edn, 2007.
3 J. Hölsä, T. Laamanen, M. Lastusaari, M. Malkamaki and P. Novak, *J. Lumin.*, 2009, **129**, 1606.
4 K. van den Eeckhout, P. F. Smet and D. Poelman, *Materials*, 2010, **3**, 2536.
5 K. van den Eeckhout, D. Poelman and P. F. Smet, *Materials*, 2013, **6**, 2789.

6 H. F. Brito, J. Hölsä, T. Laamanen, M. Lastusaari, M. Malkamäki and C. V. Lucas, *Opt. Mater. Express*, 2012, **2**, 371.
7 Y. J. Liang, F. Liu, Y. F. Chen, K. N. Sun and Z. W. Pan, *Dalton Trans.*, 2016, **45**, 1322.
8 Y. Katayama, B. Viana, D. Gourier, J. Xu and S. Tanabe, *Opt. Mater. Express*, 2016, **6**, 1405.
9 Y. Li, Y. Y. Li, K. Sharafudeen, G. P. Dong, S. F. Zhou, Z. J. Ma, M. Y. Peng and J. R. Qiu, *J. Mater. Chem. C*, 2014, **2**, 2019.
10 Y. J. Chuang, Z. P. Zhen, F. Zhang, F. Liu, J. P. Mishra, W. Tang, H. Chen, X. Huang, L. Wang, X. Chen, J. Xie and Z. Pan, *Theranostics*, 2014, **4**, 1112.
11 Q. L. M. de Chermont, C. Chaneac, J. Seguin, F. Pelle, S. Maitrejean, J. P. Jolivet, D. Gourier, M. Bessodes and D. Scherman, *Proc. Natl. Acad. Sci. U. S. A.*, 2007, **104**, 9266.
12 P. F. Smet, B. Viana, S. Tanabe, M. Y. Peng, J. Hölsä and W. Chen, *Opt. Mater. Express*, 2016, **6**, 1414.
13 F. Liu, Y. J. Liang and Z. W. Pan, *Phys. Rev. Lett.*, 2014, **113**, 177401.
14 F. Liu, Y. F. Chen, Y. J. Liang and Z. W. Pan, *Opt. Lett.*, 2016, **41**, 954.
15 T. H. Maiman, *Nature*, 1960, **187**, 493.
16 F. Liu, W. Z. Yan, Y. J. Chuang, Z. P. Zhen, J. Xie and Z. Pan, *Sci. Rep.*, 2013, **3**, 1554.
17 Z. W. Pan, Y. Y. Lu and F. Liu, *Nat. Mater.*, 2012, **11**, 58.
18 A. Bessière, S. Jacquart, K. Priolkar, A. Lecointre, B. Viana and D. Gourier, *Opt. Express*, 2011, **19**, 10131.
19 T. H. Maiman, *Phys. Rev. Lett.*, 1960, **4**, 564.
20 S. Heer, M. Wermuch, K. Kramer and H. U. Güdel, *Chem. Phys. Lett.*, 2001, **334**, 293.
21 M. Pollnau, D. R. Gamelin, S. R. Lüthi, H. U. Güdel and M. P. Hehlen, *Phys. Rev. B: Condens. Matter Mater. Phys.*, 2000, **61**, 3337.
22 International Commission on Non-Ionizing Radiation Protection, *Health Phys.*, 2013, **105**, 271.

